Hyperfine Interactions in Molecular Iodine†

M. D. Levenson* and A. L. Schawlow
Department of Physics, Stanford University, Stanford, California 94305
(Received 13 December 1971)

The hyperfine structure of eleven optical transitions in the molecules I_2^{127} and I_2^{129} was resolved by the technique of laser-saturated absorption. All the absorption lines correspond to transitions between the $^1\Sigma_g^+(X)$ and the $^3\Pi_{0u}^+(B)$ electronic states, but the rotational and vibrational quantum numbers varied widely. Two distinct types of hyperfine interaction were observed: (i) a nuclear electric quadrupole coupling which changed little among the lines investigated, and (ii) a magnetic spin-rotation interaction which varied strongly with the vibrational energy in the electronically excited state. The origin of the latter effect is discussed.

INTRODUCTION

It has long been known that absorption lines in the visible spectrum of iodine are wider than the expected inhomogeneous linewidth. The extra linewidth has generally been attributed to an unresolved hyperfine splitting due to the nuclear electric quadrupole (NEQ) interaction.[1] Recently the technique of laser-saturated absorption has been employed to resolve the hidden structure of a few of these transitions.[2,3] These studies have shown the existence of a contribution to the hyperfine splitting due to a magnetic interaction between nuclear spin and molecular rotation, in addition to the NEQ term.[4]

In the present investigation, ion lasers were employed in the Hänsch-Bordé saturated-absorption technique to survey the hyperfine splitting of iodine absorption lines in the region from 5682 to 5017 Å. In this method, two beams of equal frequency are sent in opposite directions through an external iodine-vapor absorption cell. One beam is periodically chopped and the intensity modulation of the other (probe) beam, which results from the nonlinear interaction in the absorbing gas, is detected. The transmission of the probe beam is enhanced by the saturation of the absorption produced by the other beam if the laser frequency ω is tuned close to the line center Ω_{ab} of one of the Doppler-broadened transitions (a and b refer to the two levels involved). Both light waves then interact with the same molecules, those within the narrow range of axial velocity centered at $v_z = 0$.

For moderate light intensity and large Doppler width, a simple hole-burning model is adequate to describe the transmission increase. Such a model predicts that the change of the partial absorption coefficient α_{ab} for the probe beam due to a saturating beam of intensity g is

$$\frac{\Delta\alpha_{ab}}{\alpha_{ab}} = -\frac{1}{2}\frac{g}{g_{\text{sat}}}\frac{\gamma_{ab}^2}{\gamma_{ab}^2 + (\Omega_{ab}-\omega)^2}\ , \qquad (1)$$

where γ_{ab} is the natural linewidth of the transition,[5] and

$$g_{\text{sat}}^{-1} = \frac{4\pi}{\hbar^2 c}\frac{|\mu_{ab}|^2}{3}\gamma_{ab}^{-1}(T_a + T_b - A_{ab}T_aT_b)\ . \qquad (2)$$

The saturation parameter g_{sat} depends on the matrix element μ_{ab} of the transition, on the lifetimes of the two levels involved, T_a and T_b, and on the rate A_{ab} of the direct and cascade spontaneous transitions connecting the upper and lower states.

The iodine molecule possesses many possible transitions with slightly different resonance frequencies. As long as these transitions are independent, the observed saturation spectrum will be merely a linear superposition of resonance lines as given by Eq. (1).

The 11 transitions investigated all originate in the lowest two vibrational sublevels of the ground electronic state ($^1\Sigma_g^+$ or X). The rotational quantum numbers, however, range from 10 to 117. In addition, the vibrational quantum number in the upper state ($^3\Pi_{ou}^+$ or B) varies from 17 to ~ 62, the latter state lying only 130 cm^{-1} from the dissociation limit.[6] These resolved spectra come from states sufficiently diverse that conclusions can be drawn about the variation of quadrupole and magnetic hyperfine coupling constants with the quantum numbers of the molecule.

EXPERIMENTAL PROCEDURE

Iodine has absorption lines all through the center of the visible region, but the technique of saturation spectroscopy can only be applied to transitions which happen to fall at some laser frequency (at least until broadly tunable lasers of adequate stability are developed). Thus the early experiments on iodine were performed using the 6328-Å He-Ne laser line.[2,7,8]

The krypton and argon ion lasers have, however, several advantages over the He-Ne laser for the purpose of laser-saturated-absorption spectroscopy. First, each laser produces a number of distinct

wavelengths; widely different molecular transitions may be conveniently investigated. The gain band of each line is wider, so that there is a larger chance of finding an accidental coincidence with a molecular transition at a given wavelength. The entire hyperfine structure of a given line may be more clearly observed. Finally the output power of these lasers is sufficient to permit saturated-absorption experiments to be performed outside the laser cavity even in the case of relatively weak transitions. In this investigation, at least one resolvable iodine absorption line was found at each laser wavelength.

The iodine vapor was sealed in Pyrex cells 20 cm in length. The pressure of the gas could be controlled by varying the temperature of a side tube in which crystals of the element rested. The cells were evacuated through a cold trap by a mechanical roughing pump and an oil diffusion pump. The residual pressure of foreign gases was less than 3×10^{-5} torr.

Two Coherent Radiation model 52G ion lasers were used in this work; one was filled with argon, the other with krypton. A particular laser transition was selected by a Brewster-angle prism within the cavity, and a solid quartz etalon (temperature stabilized) with 6-GHz free spectral range and 8% reflecting surfaces suppressed all but a single axial mode.

The frequency of the laser was scanned by varying the cavity length. The output mirror was supported by a piezoelectric translator that could move as much as 10 μm. Another piezoelectric actuator varied the angle of the etalon to maximize the output at each frequency. The laser could be scanned continuously over the inhomogeneously broadened linewidth of the iodine transitions in a few minutes by applying the proper voltages to the transducers.

The geometry of the experimental setup appears in Fig. 1. The output of the laser was split into two beams of roughly equal intensity by the beam splitter at S. The beams were reflected by the mirrors at A and B to cross at a small angle (< 2 mrad) within the iodine cell. One beam (the pump or saturating beam) was chopped at 1000 Hz, and a small fraction of the other (< 0.01%) monitored by a 1P28 photomultiplier. The modulation of this second (probe) beam was detected by a PAR HR-8 phase-sensitive amplifier. Serious noise resulting from fluctuations in laser power was reduced by using a 0.1-sec time constant. Spurious signals originating from the scattering of the pump beam by the windows of the cell were avoided by using a relatively strong probe beam in the cell and attenuating it at the photomultiplier.

A 1-m focal length lens placed ahead of the beam splitter reduced the diameter of the beams within the cell to $w_0 = 0.34$ mm, thus increasing the size

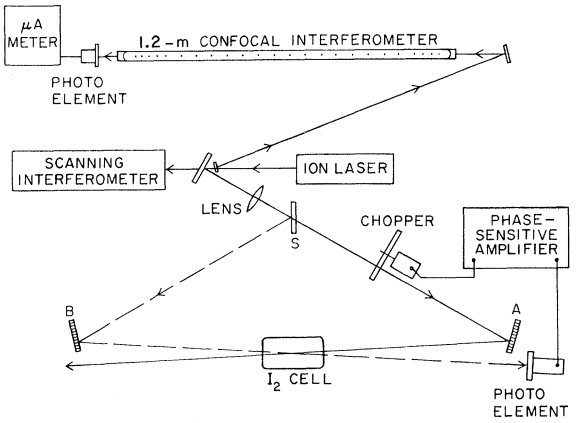

FIG. 1. Schematic diagram of the saturation spectrometer.

of the saturation signal. The pressure of the iodine vapor (determined from the known temperature and vapor pressure of the solid[9]) was varied from one run to another to ensure the maximum signal.

The laser frequency shift was not a linear function of the scanning voltage applied to the mirror transducer; an independent frequency marker was necessary to calibrate the frequency scale. The known frequency separation between the TEM_{00q} modes of a 1.2-m confocal interferometer provided this frequency reference. With aluminized mirrors and a fused-quartz spacer, this interferometer produced markers every 128.5 MHz, with an accuracy of 1 MHz.

Another confocal interferometer continuously monitored the mode structure and power output of the laser. Any malfunction or incipient mode jump was immediately detected on the face of a storage oscilloscope which displayed the output of this mode analyzer.

One x-y plotter recorded the modulation of the probe beam as a function of the voltage on the mirror translator while another plotted the transmission of the 1.2-m interferometer vs the same voltage. By changing the speed of the voltage ramp applied to the transducer, the spectrum could be scanned at any desired rate while maintaining the same linear scale on the plotter traces.

Slow drifting of the laser frequency (due perhaps to thermal expansion of the resonator structure) merely added to the scanning rate. Such drifts were roughly linear and did not result in error. More serious were small rapid jumps in the laser frequency due to the sudden release of strains caused by thermal expansion. These jumps in laser frequency and the slight thermal changes in the length of the interferometer limited the accuracy to which frequency differences could be measured. Because of these small but irregular jumps, the quadrupole

coupling constants were measured with uncertainties ranging from 10 to 17 MHz, even though the lines were as narrow as 5 to 10 MHz or about 10^{-8} of the light frequency.

Most of the lines were investigated in linearly polarized light, but some of the later work involving an argon laser utilized circularly polarized light. No difference in the spectra was noted; but since the laser could be isolated from optical feedback when circularly polarized light was used, alignment was simpler in the latter case.

Typically, the laser produced output power of the order of 30 mW, with each of the two beams through the cell measuring 6 mW, and the monitors and reflection loss accounting for the rest. The laser intensity within the cell was ~ 2.5 W/cm^2, much less than the value of the saturation intensity, which for a typical transition was ~ 15 W/cm^2. In the case of the strong 5145-Å line of argon, the probe beam was 1.6 mW and the pump 6 mW; an attenuator was employed in each beam to avoid power broadening.

The frequencies of the hyperfine components on each trace were determined relative to that of an arbitrarily chosen zero component by interpolation between the nearest four interferometer peaks with a cubic polynomial. The splittings between each succeeding pair of lines were similarly determined and tabulated.

The states between which the transition occurred were identified from the fluorescence spectrum of the excited iodine vapor. The laser frequency excites the molecules into a particular rotational vibrational sublevel of the B electronic state (characterized by the quantum numbers J' and v'). The selection rule for radiative decay is the same as for absorption: $\Delta J = \pm 1$. The fluorescence spectrum thus consisted of pairs of lines, the splitting within each pair given by

$$\Delta\nu = B_{v''}(4J' + 2) \quad . \tag{3}$$

The intervals between the pair were given by the vibrational frequency of the lower electronic state.[10]

The laser frequency falls on one component of such a pair of lines. If it is at the high-frequency member, then the selection rule for the *absorption* is $J' - J'' = +1$, and the absorption corresponds to an R-branch line. If the laser falls on the low-frequency component, the selection rule is $J' - J'' = -1$, and a P-branch assignment is made. The vibrational quantum number in the lower electronic state (v'') was assigned from the number of anti-Stokes fluorescence lines.[2]

The doublet splitting of a convenient pair of lines (generally those that fell nearest the laser frequency) was measured with a 1-m Ebert scanning monochromator. The resolution (0.16 cm^{-1}) was sufficient to determine J' to within ± 1. The number of components in the hyperfine spectrum indicated whether J'' was even or odd. The frequency scale was defined by pairs of emission lines of known wavelength from a sodium or helium-neon lamp.[11] With the other quantum numbers determined, v' can be assigned from a knowledge of the laser frequency and the molecular constants.[10,6] Usually, only one transition with the other three quantum numbers correct will fall near the laser line. The accuracy with which the frequencies of given transitions can be predicted is rather poor, especially for $v' > 43$. A mistake in the identification of one band makes the most recent molecular constants useless in this region.[12,13] Constants for I_2^{129} were estimated using the usual isotope-effect formulas.[14] The value of v' for the 5017-Å transition was assigned using band-head data.[15]

INTERPRETATION

The rotational vibrational levels of both the $^1\Sigma_g^+$ (X) and the $^3\Pi_{ou}^+(B)$ electronic states are split by hyperfine interactions. In terms of the nuclear-spin vectors $\vec{I}_1$ and $\vec{I}_2$ and the rotational angular momentum vector $\vec{J}$, the Hamiltonian for the nuclear electric quadrupole interaction is[16]

$$\mathcal{H}_{\mathrm{NEQ}} = -eQq\left(\frac{3(\vec{I}_1\cdot\vec{J})^2+\frac{3}{2}(\vec{I}_1\cdot\vec{J})-|\vec{I}_1|^2|\vec{J}|^2}{2(2J+3)(2J-1)I_1(2I_1-1)}\right.$$
$$\left.+\frac{3(\vec{I}_2\cdot\vec{J})^2+\frac{3}{2}(\vec{I}_2\cdot\vec{J})-|\vec{I}_2|^2|\vec{J}|^2}{2(2J+3)(2J-1)I_2(2I_2-1)}\right). \tag{4}$$

Similarly the magnetic spin-rotation interaction is given by[4]

$$\mathcal{H}_M = (\mu G/I_1)(\vec{I}_1+\vec{I}_2)\cdot\vec{J} \quad . \tag{5}$$

Various conventions for the coupling constants eQq and $\mu G/I_1$ appear in the literature.[3,4,8] Except where specifically noted, the field gradient q discussed in this paper is measured along the internuclear axis of the molecule. The values quoted must be divided by $-(2+3/J)$ to convert them to the system where the field gradient is measured along the direction of the rotational angular momentum.[16,17] The spin-rotation coupling $\mu G/I_1$ has also been quoted as C and $K/J(J+1)$. Since this work treats both natural iodine (atomic weight 127) and a radioactive isotope (atomic weight 129) with different spin and moments, it seemed wise to include the dependence on the nuclear parameters in the definition of the coupling constants. The spin and moments of the I^{127} nucleus are $I_1 = \frac{5}{2}$, $Q = -0.79$ b, and $\mu = 2.808\mu_N$. For I^{129} the parameters are $I_1 = \frac{7}{2}$, $Q = -0.55$ b, and $\mu = 2.617\mu_N$.[18]

The Pauli exclusion principle requires that the total wave function of a homonuclear diatomic molecule with half-integer nuclear spin be antisymmetric under exchange of the nuclei. In a state of even (*gerade*) electronic symmetry, such as the X state of iodine, only states of odd total nuclear spin

($I=1$, 3, 5 and, for I_2^{129}, 7) can combine with odd-J states, and states of even nuclear spin ($I=0$, 2, 4 and, for I_2^{129}, 6) can combine only with even-J states. Since the total number of hyperfine states with nuclear spin I is $2I+1$, states of even J have fewer hyperfine components than those with odd J. For an odd (*ungerade*) electronic state such as the B state, the I, J combination rules are reversed.[1]

Energy levels are obtained by diagonalizing the submatrices of the energy matrix calculated by the method of Robinson and Cornwall in the $I_1\, I_2\, I\, J\, F\, M_F$ representation. The eigenvalues are then labeled by the quantum numbers $I_1\, I_2\, \epsilon\, J\, F$. The pseudospin quantum number ϵ corresponds to the value of I that makes the largest contribution to the eigenstate.

For large values of J, the hyperfine splitting can be approximated by a rather simple model. For $J \gg I_1$ the rotational angular momentum vector is almost parallel to $\vec{F}$. It may be treated as having a fixed direction in space, and the projections of the nuclear angular momenta may be quantized independently along this axis. Introducing the quantum numbers M_1 and M_2,

$$\begin{aligned} F_1 &= J + M_1, & \vec{F}_1 &= \vec{J} + \vec{I}_1 , \\ F_2 &= J + M_2, & \vec{F}_2 &= \vec{J} + \vec{I}_2 , \\ -I_1 &\le M_1 \le I_1, & -I_1 &\le M_2 \le I_1 , \end{aligned} \tag{6}$$

we have approximately

$$\begin{aligned} (\vec{I}_1 \cdot \vec{J}) &= M_1 J + \tfrac{1}{2}[M_1(M_1+1) - I_1(I_1+1)], \\ (\vec{I}_1 \cdot \vec{J})^2 &= M_1^2 J^2 + M_1 J[M_1(M_1+1) - I_1(I_1+1)] + O(I_1^4) , \\ (\vec{I}_2 \cdot \vec{J}) &= M_2 J + \tfrac{1}{2}[M_2(M_2+1) - I_1(I_1+1)], \\ (\vec{I}_2 \cdot \vec{J})^2 &= M_2^2 J^2 + M_2 J[M_2(M_2+1) - I_1(I_1+1)] + O(I_2^4) . \end{aligned} \tag{7}$$

A substitution of these quantities into (4) and (5) yields the approximate energy levels

$$E_{\mathrm{NEQ}} \approx -\frac{eQq}{8I_1(2I_1-1)}\left(3(M_1^2+M_2^2) + (3/J)\{M_1[M_1(M_1+1) - I_1(I_1+1) + \tfrac{1}{2}] + M_2[M_2(M_2+1) - I_1(I_1+1) + \tfrac{1}{2}]\} - 2I_1(I_1+1)\right), \tag{8}$$

$$E_M \approx (\mu G/I_1)(M_1+M_2)J \ .$$

The Pauli principle forbids the nuclear-spin states where $M_1 = M_2$ from combining with symmetric molecular wave functions.

The coupling coefficients eQq and $\mu G I^{-1}$ are not directly measured in a spectroscopy experiment. The selection rules for the electronic transition are $\Delta\epsilon = 0$, $\Delta F = \Delta J = \pm 1$ (or for large J, $\Delta M_1 = \Delta M_2 = 0$).[4,16] These selection rules prevent transitions between dissimilar nuclear-spin states. In the transitions resolved here, only the hyperfine coupling constants—not the nuclear-spin wave functions—change. The resolved structure corresponds to the differences between the hyperfine energies of sublevels of the two electronic states which have the same quantum numbers ϵ and $F-J$ (or M_1 and M_2 for large J). Thus only the differences between the constants in the two states,

$$\begin{aligned} \Delta eQq &= eQq^1 - eQq^0, \\ \frac{\mu G_{\mathrm{expt}}}{I_1} &= \frac{\mu}{I_1}(G^1 - G^0) \ , \end{aligned} \tag{9}$$

are directly measurable. The splitting of a resonance line approximates that of a rotational vibrational level with the same J as the lower state and hyperfine coupling constants equal to ΔeQq and $(\mu/I)G_{\mathrm{expt}}$ (see Figs. 2 and 3).

The observed spectra were divided into two classes: those where the frequencies were given within the experimental error by evaluating the Hamiltonian in Eqs. (4) and (5) to first order, and those in which the second-order NEQ contributions were significant.[7,19] In practice, any line with $J > 20$ fell into the former class, while those with $J \le 20$ fell in the latter. Kroll's calculations[19] show that the second-order contributions are of order 1 MHz or less for $J = 10$ and are roughly proportioned to $J^{-3/2}$.

In either case, the coupling constants were determined by minimizing the root-mean-square deviation of the frequencies and splittings calculated with Eqs. (4) and (5) from the observed values. The coefficients thus determined appear in Tables I and II.[5] The field gradient in the ground electronic state was assumed to be $eq^0 = 3600$ MHz/b; the spin-rotation coefficient in the lower state (e.g., G^0) was assumed to vanish.

The difference in quadrupole field gradients $eq' - eq^0$ (calculated by dividing the experimental value of ΔeQq by the known nuclear quadrupole moment Q) varied little among the transitions. It has been predicted that the field gradient should depend upon the "spring constant" for internuclear vibrations.[20] Since the effective vibrational frequency in the B state varies quite rapidly with energy, such a model would predict a strong negative correlation between the frequency and field gradient. Figure 4, however, shows that the variation with vibrational fre-

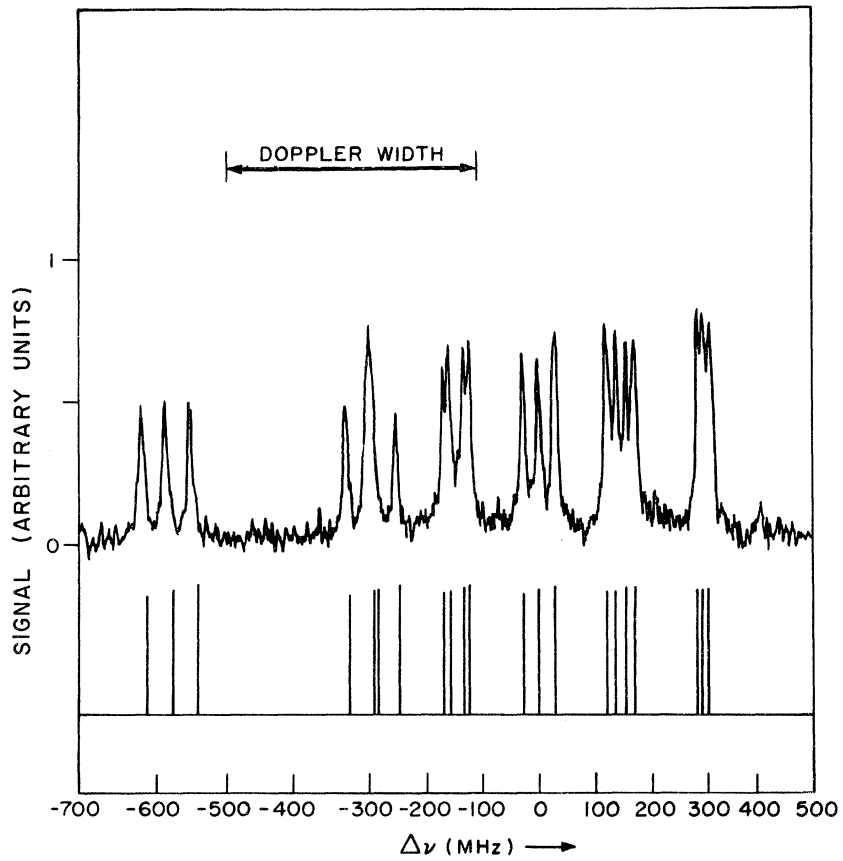

FIG. 2. Hyperfine splitting of the $P(117)$ 21-1 line in I_2^{127}.

quency is weak, and with the wrong sign.

The observed nearly constant value of $eq' - eq^0$ is better explained by the Townes-Dailey approximation.[21] The field gradient in the molecule is then related to that in the appropriate atomic state. Since the B state dissociates into two atoms, one in the $^2P_{3/2}$ state and the other in the gradient free $^2P_{1/2}$ state, the field gradient in the B state could be expected to approximate a constant half of the atomic value.[22,23]

SPIN-ROTATION INTERACTION

For states where $J > 20$, the deviations of the observed structure from a pure quadrupole spectrum are due to the spin-rotation interaction. The coupling coefficient G_{expt} showed no dependence upon the rotational quantum number J (at least for the large J lines), but varied dramatically with the vibrational energy in the upper state. Figure 5 is a plot of G_{expt} vs the vibrational energy. The solid line is the graph of the empirical formula

$$G_{\text{expt}} \simeq \frac{1.2\times10^5}{4400-E} - 12.5 \text{ kHz}/\mu_N \ , \qquad (10)$$

where E is the vibrational energy of the upper state in cm^{-1}.

An energy dependence of this sort would be expected if the magnetic hyperfine interaction in the B state were due to a coupled electronic state lying about 4400 cm^{-1} above the minimum of the B-state potential (see Fig. 6).[23,24] In zeroth order, the nuclei in a molecule in a $^1\Sigma$ or a $^3\Pi_0$ electronic state experience no average magnetic field in the $\vec{J}$ direction. The end-over-end rotation of the molecule can, however, couple excited electronic states with

TABLE I. Parameters of the resolved transitions.

λ(Å)	Isotope 127	Isotope 129	Transition	ΔeQq (MHz)	$\mu G_{\text{expt}} I^{-1}$ (kHz)
6328	X		$P(33)$ 6-3[a]	1938 ± 0.3	21.6 ± 1
6328	X		$R(127)$ 11-5[b]	1926 ± 3	28 ± 2
5682		X	$P(20)$ 17-0	1356 ± 12	27 ± 9
5682	X		$P(117)$ 21-1	1936 ± 17	49 ± 4
5308	X		$P(10)$ 32-0	1920 ± 17	60 ± 40
5308	X		$R(13)$ 32-0	1920 ± 16	40 ± 30
5208		X	$R(71)$ 40-0	1307 ± 10	98 ± 3
5208	X		$R(78)$ 40-0	1888 ± 16	152 ± 6
5145	X		$P(13)$ 43-0	1890 ± 16	210 ± 30
5145	X		$R(15)$ 43-0	1890 ± 16	150 ± 30
5145		X	$R(109)$ 51 ± 1-0	1292 ± 10	244 ± 2
5145		X	$R(67)$ 53 ± 1-1	1299 ± 10	265 ± 3
5017	X		$R(26)$ 62-0	1875 ± 16	944 ± 18

[a]Bunker, Hanes, and co-workers.
[b]Hanes and Dahlstrom.

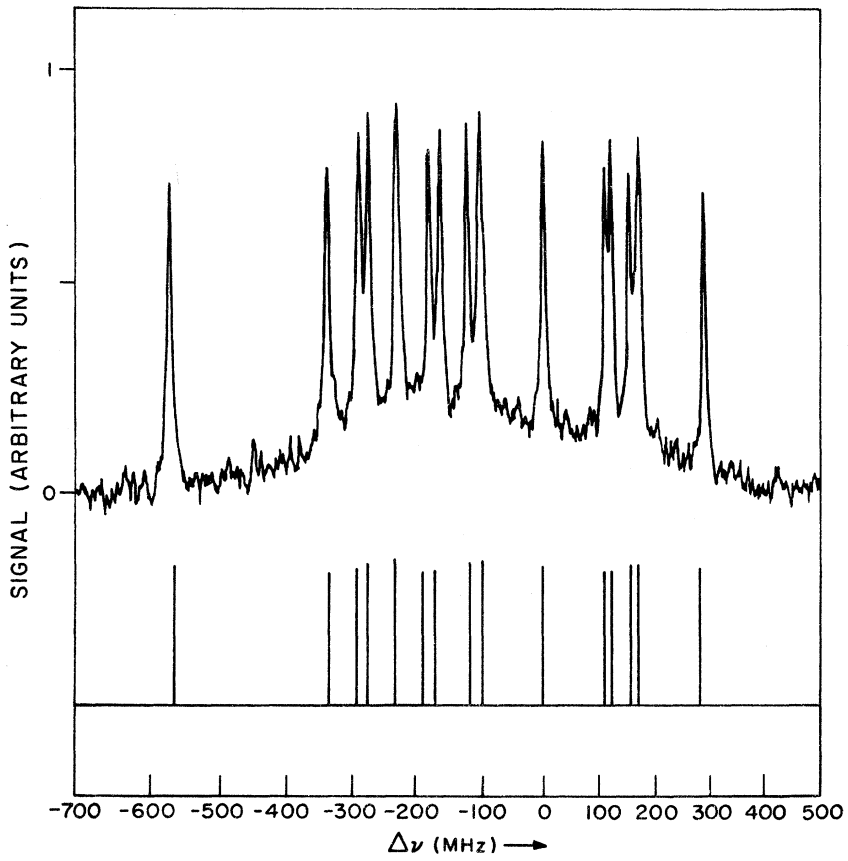

FIG. 3. Hyperfine splitting of the $R(78)$ 40-0 line in I_2^{127}.

the zeroth-order state. Thus there can be a small net component of electronic angular momentum and magnetic field along the J axis:

$$\langle 0|\vec{J}_e|0\rangle^1 = 4\pi\hbar B \sum_n \frac{|\langle n|J_e|0\rangle|^2}{E_n - E}\ \vec{J} \quad . \tag{11}$$

This explanation for the magnetic hyperfine interaction has often been applied to molecules with $^1\Sigma$ ground electronic states. The B state of iodine is, however, a $^3\Pi_0$, and care must be taken to properly include the effects of electronic spin. The electronic angular momenta in the iodine molecule couple according to Hund's case (c), [23] and the spin-rotation interaction is given by[24]

$$\mathcal{H}_M = \frac{\mu_I}{I}\ 8\pi\hbar B \left((g_J a + g_s b) \sum_n \frac{|\langle 0|J_{ex}|n\rangle|^2}{E_n - E_0} \right.$$

TABLE II. Parameters of the energy states.

J'	V'	E (cm^{-1})	$\omega_{v'}$ (cm^{-1})	Δeq (MHz/b)	G_{expt} (kHz/μ_n)	$10^6\ G_{expt}/B$ (μ_n^{-1})
32	6	780	115	−2453 ± 0.4	19.0 ± 1	23 ± 1
128	11	1340	106	−2438 ± 3.8	25.0 ± 2	31 ± 2
19[a]	17	1940	95	−2465 ± 22	36 ± 12	47 ± 16
116	21	2320	88	−2451 ± 21	44.0 ± 5	58.4 ± 7
9	32	3170	65	−2430 ± 21	53.4 ± 36	79.8 ± 53.8
14	32	3170	65	−2430 ± 20	35.6 ± 27	53.2 ± 40.3
72[a]	40	3620	48	−3290 ± 20	131 ± 4	224 ± 7
79	40	3630	48	−2376 ± 18	135 ± 5	231 ± 9
12	43	3770	42	−2392 ± 20	187.0 ± 27	336.9 ± 49
16	43	3770	42	−2392 ± 20	135.5 ± 27	246.5 ± 49
110[a]	51 ± 1	4030	25	−2349 ± 18	333 ± 3	775 ± 7
68[a]	53 ± 1	4080	21	−2362 ± 18	354 ± 4	849 ± 9
27	62	4260	12	−2373 ± 20	841 ± 15	2570 ± 46

[a] I_2^{129}.

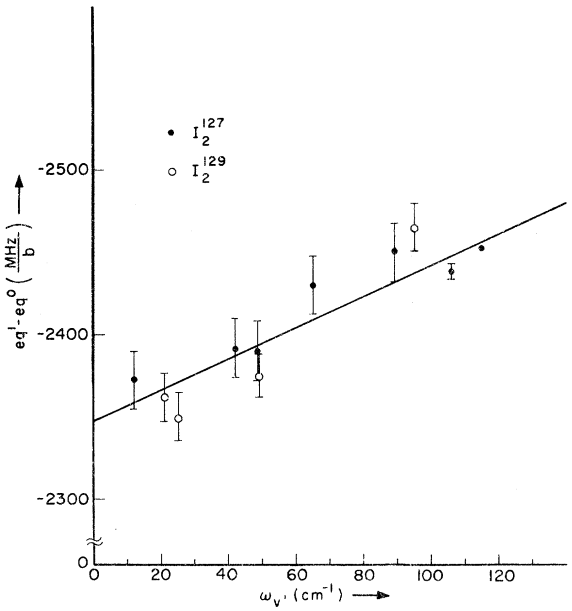

FIG. 4. Experimentally determined difference of the electric field gradients between the B and X electronic states as a function of the vibrational frequency in the B state, measured in cm^{-1} (3×10^{10} Hz).

$$-\pi\frac{z_e e}{cR\hbar}\Big)\vec{I}_i\cdot\vec{J}\ , \quad (12)$$

where μ_I is the nuclear magnetic moment; $B=\hbar/4\pi A_x$ is the rotational constant; A_x is the molecular moment of inertia about an x axis perpendicular to the internuclear line;

$$a=2\mu_B\langle 1/r^3\rangle_{av}$$

and

$$b=2\mu_B\left\langle\frac{8\pi}{3}\psi^2(0)-\frac{3\cos^2\theta-1}{2r^3}\right\rangle_{av}$$

are averaged over the valence electrons; $\psi^2(0)$ is the valence electron density at the nucleus; R is the internuclear distance; θ is the angle between $\vec{J}$ and the radius vector $\vec{r}$ from the nucleus to the electron; J_{ex} is the electronic angular momentum component along the x axis; and the g factors are

$$g_s=\frac{2\vec{S}\cdot\vec{J}_e}{J_e(J_e+1)} \quad \text{and} \quad g_L=\frac{\vec{L}\cdot\vec{J}_e}{J_e(J_e+1)}\ .$$

The sum in Eq. (12) is over all states of the molecule. Applying the Born-Oppenheimer approximation, one may separate the matrix element into nuclear and electronic parts: $|\langle n|J_e|0\rangle|^2=|\langle k|J_e|0\rangle|^2\times|\langle\phi_k(E_k)|\phi(E)\rangle|^2$. The second factor is simply the Franck-Condon overlap factor between nuclear wave functions in the two electronic states with energies E and E_k. If only one electronic state contributes to the sum, one may write

$$\sum_n\frac{|\langle n|J_e|0\rangle|^2}{E_n-E}=|\langle 1|J_e|0\rangle|^2\times\int\frac{|\langle\phi_1(E_1)|\phi(E)\rangle|^2}{E_1-E}\rho(E_1)\,dE_1$$

$$=\frac{|\langle 1|J_e|0\rangle|^2}{E'-E}\ , \quad (13)$$

where $\rho(E_1)$ is the density-of-states factor, and the last equality defines E'.

The spin-rotation constant is then given by

$$G=4B_v\left((g_J a+g_s b)\frac{|\langle 1|J_{ex}|0\rangle|^2}{E'-E}-\frac{Z_e e}{cR\hbar}\right)\ \text{Hz}/\mu_N\ . \quad (14)$$

Only certain states (those where the nuclear wave functions in the two electronic levels overlap significantly) contribute to the spin-rotation interaction. This implies that the average interatomic spacing, and therefore the rotational constants, for the two

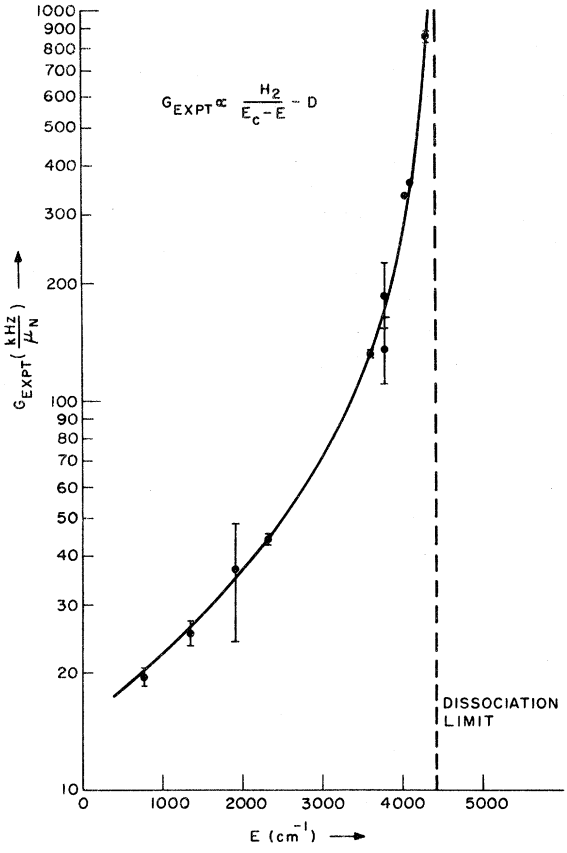

FIG. 5. Observed difference in spin-rotation coupling coefficients as a function of the vibrational energy in the electronically excited state.

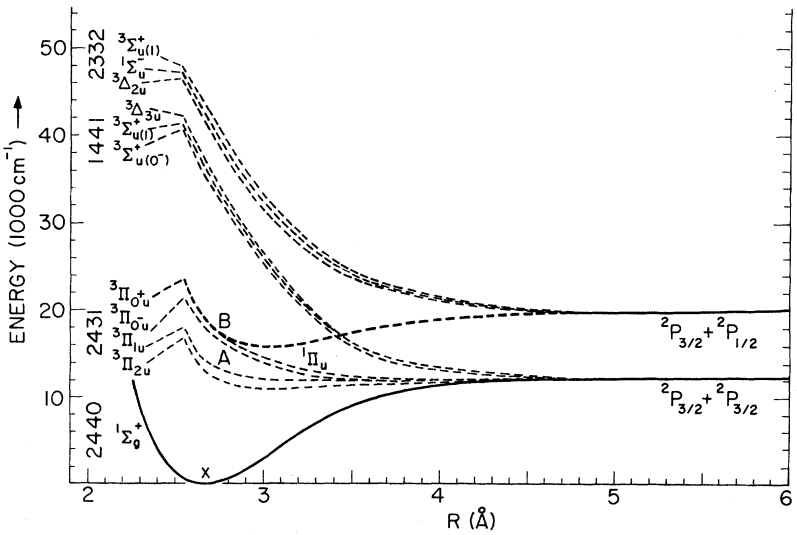

FIG. 6. The electronic energy-level structure of iodine near the B and X states. The four numbers at the left give the configuration of the valence electrons; the notation $wxyz$ implies that the state is $\sigma_u^2\sigma_g^2\sigma_g^w\pi_u^x\pi_g^y\sigma_u^z$. All states of *gerade* symmetry except the ground state have been deleted (Ref. 23).

states coupled by the perturbation are roughly equal. Since total angular momentum is conserved, the contributions of the rotational energy to E and E' in Eq. (11) cancel. The energy E in Eq. (13) is then just the vibrational energy of the state involved.

The spin-rotation coupling coefficient resulting from this mechanism is independent of the rotational quantum number J. Other types of magnetic hyperfine interaction applicable to $^3\Pi_0$ electronic states produce coupling constants which are strong functions of J.[25] No evident correlation between G_{expt} and J appears in our data, but there is indeed a strong variation with the vibrational energy.

Both states connected by the various optical transitions may have a spin-rotation interaction of this type. The observed magnetic splitting should then obey an equation of the form

$$\frac{G_{\text{expt}}}{B_{v'}} \simeq \frac{L^2}{E_c - E} - D \ , \tag{15}$$

where $L^2 = 4(g_J a + g_s b)|\langle 1|J_e|0\rangle|^2$, and $D = \pi(Z_e e/cR\hbar) + B_v^{-1} G^0$, accounts both for the nuclear contribution and a possible spin-rotation coupling in the lower state. Figure 7 is a plot of the observed coupling constant; the solid line is a function of the form in Eq. (15). The parameters that best fit the data are

$$D = (40 \pm 10) \times 10^{-6}\ \mu_N^{-1} \ ,$$

$$E_c = 4340 \pm 40\ \text{cm}^{-1} \ ,$$

$$L^2 = 0.22 \pm 0.02\ \text{cm}^{-1}/\mu_N \ .$$

Since the nuclear contribution to the constant D is only $1.5 \times 10^{-6}\ \mu_N^{-1}$ (assuming an effective nuclear charge of $z_e = 5$), one might estimate that the spin-rotation constant G^0 in the ground electronic state of I_2 is $G^0 \simeq 33 \pm 9$ kHz/μ_N. This estimate must, however, be regarded as an upper limit; since E' is not really a constant and might well increase with decreasing v', part of the deviation of G_{expt} from a simple $1/(E' - E)$ law is likely due to another mechanism.

Figure 6 shows the internuclear potentials of some of the low-lying electronic states of I_2. Since the energy E' is so close to the binding energy of the B state ($D_e = 4391 \pm 20\ \text{cm}^{-1}$),[6] one of the three

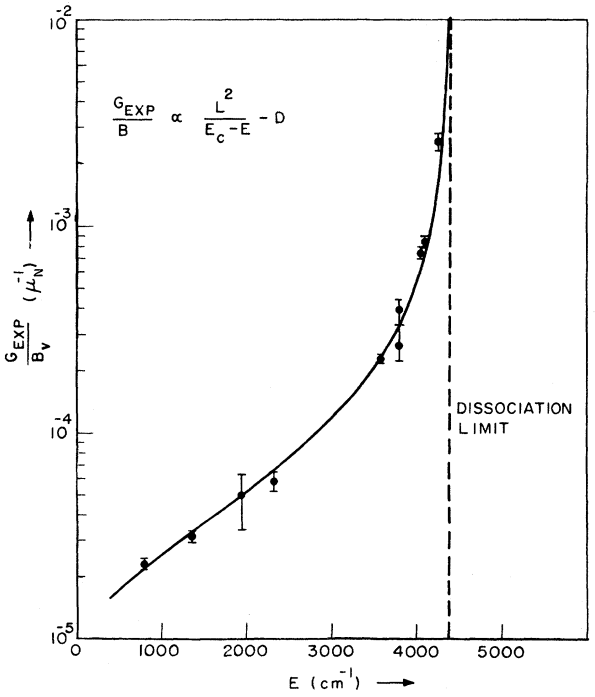

FIG. 7. Comparison of the experimental and theoretical energy dependence of the spin-rotation coupling parameter.

ungerade states of the 2332 configuration in Fig. 6 probably causes the spin-rotation coupling.[23,24] Were any of the other states involved (e.g., the $^1\Pi$), the parameter E' would be significantly smaller.

Finally it is interesting to use Eqs. (11) and (14) to estimate the total projection of J_e along the direction of J. If the contribution to the molecular magnetic field due to the electronic spins is ignored ($g_s = 0$, $g_L = 1$), the parameter a in Eq. (14) may be approximated by[24,26]

$$a = \mu_B \langle 1/r^3 \rangle_{at} = \mu_B (18/a_0^3) \ ,$$

where a_0 is the Bohr radius. For our largest value of G_{expt}, the average projection of electronic angular momentum in the J direction is $\langle 0|J_e|0\rangle \simeq 0.03\hbar$.[1] Even at an energy only 130 cm^{-1} from the dissociation limit, the B state of I_2 remains a good example of Hund's case (c) with little admixture of case (e). If the energy dependence of $\langle 0|J_e|0\rangle$ continues as expected, however, the molecule may well convert to a case-(e) configuration at an energy below the dissociation limit. The well-known disappearance of discrete absorption lines near the dissociation limit might be one consequence of this transformation.[6]

LOW-J LINES

The shifts in the resonance frequencies due to the spin-rotation interaction are rather small for transitions with J values less than roughly 20. The spin-rotation coupling coefficient cannot be accurately determined for a transition between states with small values of J. The contributions due to the second-order NEQ effect, however, increase, and the transition frequencies become a function of the quadrupole-coupling coefficients in each state independently, not just of their difference. A trace of the hyperfine structure of two such transitions appears in Fig. 8. A comparison of the hyperfine-structure patterns of the two absorption lines, however, permits an estimate of the quadrupole coupling in the ground electronic state.

The electric field gradient along the molecular axis q is independent of the rotational quantum number J, but the corresponding quantity defined in the $\vec{J}$ direction q_J is not constant.[17] The difference in coupling coefficients defined in terms of q_J between the upper and lower state is

$$\Delta eQq_J = \frac{-eQq^1}{2+(3/J')} - \frac{-eQq^0}{2+(3/J)} \ , \qquad (16)$$

where $J' = J+1$ for R-branch lines, and $J' = J-1$ for P-branch lines.

If ΔeQq_J is determined for two transitions belonging to the same vibrational band (and having the same values of eQq' and eQq^0), but differing in their rotational quantum numbers, eQq' can be eliminated and eQq^0 calculated using Eq. (16). Since ΔeQq_J is not perfectly determined and the coefficient of eQq^0 is not large, the estimate of eQq^0 will have significant error.

Two pairs of suitable lines occurred at ion-laser frequencies, the $P(10)R(13)$ 32-0 pair at 5308 Å and the $P(13)R(15)$ pair at 5145 Å. The parameter ΔeQq_J for these lines is tabulated in Table III.

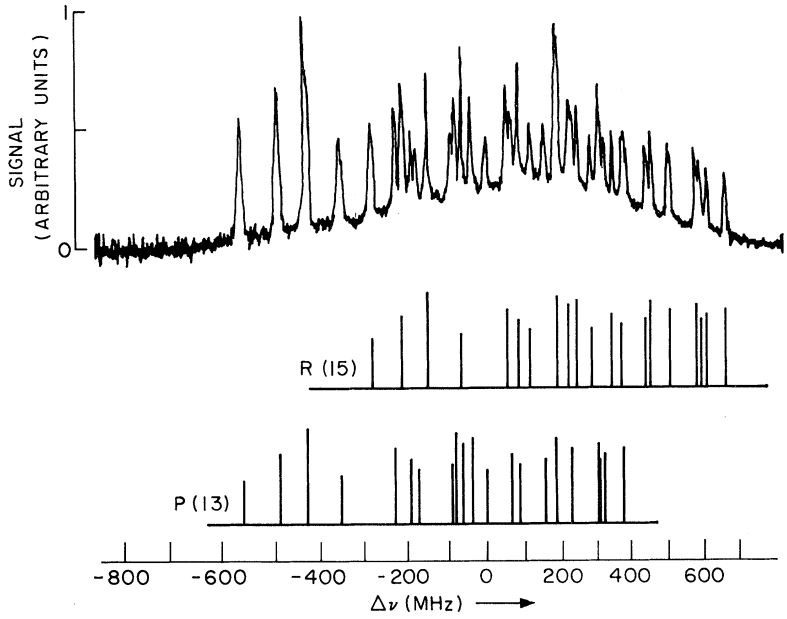

FIG. 8. The hyperfine structure of a typical pair of absorption lines with small values of J. This structure is the $P(13)$ $R(15)$ pair of lines in the 43-0 band of I_2^{127}. The transition falls within the gain of the strong 5145Å argon-laser line.

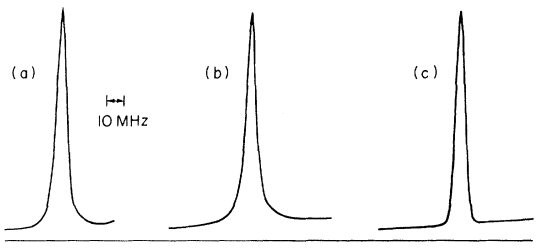

FIG. 9. (a) The experimental line shape of the hyperfine components of the $P(13)$ 43-0 transition, (b) a Lorentzian of 7.5 MHz width superimposed on a rising background, (c) a Gaussian with the same width. The Lorentzian is essentially identical with the observed line shape.

Applying Eq. (15) and eliminating ΔeQq, one obtains

$$eQq^0 = -2763 \pm 400 \text{ MHz} \quad (32\text{-}0),$$

$$eQq^0 = -2577 \pm 350 \text{ MHz} \quad (43\text{-}0),$$

(50% confidence) as estimates of the quadrupole coupling in the lower electronic state, for I_2^{127}. Although these estimates are rather rough, they agree with one that has been made from the hyperfine structure of an iodine transition at 6328 Å[7] and those made by extrapolating from the solid.[21]

LINE SHAPE

The apparatus used in this investigation was not well suited to precise investigations of the line shape of the individual hyperfine components. These structures were quite narrow in comparison with the splitting due to the hyperfine interaction. A slight jump in the frequency of the laser could badly distort the line shape while producing no detectable effect upon the splittings. Nevertheless, some interesting features were noted.

First, the components were distinctly Lorentzian (at least when the laser behaved) with strong "wings" which decreased as $1/\omega^2$ (see Fig. 9). The linewidths of all the components of a given rotational vibrational line were equal, but different lines had widths differing by as much as a factor of 2. The widths were several times too large to be explained by the known decay rate of the B state.[27,28]

These very narrow lines, achieved when Doppler broadening is eliminated by the saturation method, are sensitive, however, to collisional effects.[28] At the relatively high densities used in this investigation, pressure broadening causes most of the linewidth. Indeed, the measured widths of the resonance lines did correlate with the vapor pressure of the iodine. In addition a broad collisional background was visible in most of the spectra.[29]

Further experiments using more stable lasers and better noise-reduction techniques will be needed to clarify the experimental situation. A full understanding of the line-shape problem in saturated absorption can only come after detailed experimental and theoretical studies of a variety of physical systems.

CONCLUSIONS

In this experiment we have shown that the nuclear electric quadrupole coupling coefficient is nearly constant for a given electronic state of a molecule, even if the vibrational frequency of that state varies rapidly with energy. The difference between the quadrupole field gradients for the B and X states of iodine was found to be approximately -2400 MHz/b; a decrease in magnitude of only ~ 100 MHz/b occurred as the vibrational energy in the B state increased. The field gradient was estimated as $eq^0 = 3400 \pm 400$ MHz/b in the X state and $eq^1 = 1000 \pm 400$ MHz/b in the B state.

The B state showed a large spin-rotation interaction which increased rapidly near the dissociatior limit. The coupling coefficient G_{expt} which gives the observed hyperfine splitting of a transition due to this mechanism obeyed the phenomenological formula

$$G_{\text{expt}} \approx \frac{1.2\times 10^5}{4400 - E} - 12.5 \text{ kHz}/\mu_N , \qquad (10)$$

where E is the vibrational energy of the upper level in cm^{-1}. The spin-rotation coupling constant in the ground electronic state could only be estimated as $G^0 \leq 34 \pm 9$ kHz/μ_N. There was no correlation between the rotation coupling parameter and the rotational quantum number.

We have also demonstrated that the Hänsch-Bordé crossed-beams saturation technique yields as high resolution as the more conventional inverted Lamb dip method.[30] The lasers employed performed adequately in spite of the mechanical vibration that is unavoidable in an ion laser. Previous estimates of the fundamental limit on the short-term frequency stability imposed by this vibration

TABLE III. The parameter ΔeQq_J for the $P(10)R(13)$ 32-0 pair at 5308 Å and $P(13)R(15)$ pair at 5145 Å.

Transition	ΔeQq_J (MHz)
$P(10)$ 32-0	-838.6 ± 3.6
$R(13)$ 32-0	-856.6 ± 3.3
	50% confidence
$P(13)$ 43-0	-848.6 ± 3.3
$R(15)$ 43-0	-856.0 ± 3.3

were of the order of 20 MHz.[31] In this experiment, no recurrent instability larger than 2 MHz could be detected. Thus, in future high-resolution experiments, ion lasers may be used with some confidence. Equipped with feedback circuitry to fix its frequency at that of some iodine hyperfine component, such a laser would make a useful standard of length or frequency.

ACKNOWLEDGMENTS

The authors would like to thank Dr. R. S. Mulliken, Dr. T. W. Hänsch, and Dr. M. Kroll for several helpful discussions and M. S. Sorem, S. M. Curry, and Miss N. F. Matsuda for their considerable assistance with parts of the experiment.

---

*Present address: Gordon McKay Laboratory, Harvard University, 9 Oxford Street, Cambridge, Mass. 02138.

†Work supported by the National Science Foundation under Grant No. GP-28415.

[1]M. Kroll and K. K. Innes, J. Mol. Spectry. 36, 245 (1970).

[2]G. R. Hanes and C. E. Dahlstrom, Appl. Phys. Letters 14, 362 (1969).

[3]T. W. Hänsch, M. D. Levenson, and A. L. Schawlow, Phys. Rev. Letters 26, 946 (1971).

[4]M. Kroll, Phys. Rev. Letters 23, 631 (1969).

[5]M. D. Levenson, thesis, M. L. Report No. 2015 (Stanford University, 1971) (unpublished).

[6]J. I. Steinfeld, R. N. Zare, L. Jones, M. Lesk, and W. Klemperer, J. Chem. Phys. 42, 25 (1965).

[7]G. R. Hanes, J. Lapierre, P. R. Bunker, and K. C. Shotton, J. Mol. Spectry. 39, 506 (1971).

[8]J. P. Knox and Y. H. Pao, Appl. Phys. Letters 18, 360 (1971).

[9]*International Critical Tables of Numerical Data, Physics, Chemistry, Technology*, edited by E. W. Washburn (McGraw-Hill, New York, 1928), Vol. III, p. 201.

[10]D. H. Rank and B. S. Rao, J. Mol. Spectry. 13, 34 (1964).

[11]J. L. Rapier, H. H. Heimple, and A. L. Schawlow, Am. J. Phys. 35, 890 (1967).

[12]J. I. Steinfeld, D. S. Campbell, and N. I. Weiss, J. Mol. Spectry. 29, 204 (1969).

[13]R. J. Leroy, J. Chem. Phys. 52, 2678 (1970), note 4, p. 2682.

[14]J. L. Dunham, Phys. Rev. 41, 721 (1932).

[15]W. G. Brown, Phys. Rev. 38, 710 (1931).

[16]G. W. Robinson and C. D. Cornwall, J. Chem. Phys. 21, 1436 (1953).

[17]A. L. Schawlow and C. H. Townes, *Microwave Spectroscopy* (McGraw-Hill, New York, 1955), p. 149 ff.

[18]*Nuclear Data Tables* (Academic, New York, 1969), Sec. A, Vol. 5, p. 451.

[19]W. H. Flygare and W. P. Gwinn, J. Chem. Phys. 36, 787 (1962). We are indebted to Dr. Marvin Kroll of the University of Southern California for performing these second-order calculations for us.

[20]A. B. Anderson, N. C. Handy, and R. G. Parr, J. Chem. Phys. 50, 3634 (1969).

[21]B. P. Dailey and C. H. Townes, J. Chem. Phys. 20, 35 (1952).

[22]E. A. C. Lucken, *Nuclear Quadrupole Coupling Constants* (Academic, New York, 1969), p. 120 ff.

[23]R. S. Mulliken, J. Chem. Phys. 55, 288 (1971).

[24]R. L. White, Rev. Mod. Phys. 27, 274 (1954).

[25]K. H. Freed, J. Chem. Phys. 45, 1714 (1966).

[26]W. V. Smith and R. G. Barnes, Phys. Rev. 93, 95 (1954).

[27]K. Sakurai, G. Capelle, and H. P. Broida, J. Chem. Phys. 54, 1220 (1971).

[28]K. C. Shotton and G. D. Chapman, J. Chem. Phys. 56, 1012 (1972).

[29]P. W. Smith and T. W. Hänsch, Phys. Rev. Letters 26, 740 (1971).

[30]J. L. Hall, Institute for Theoretical Physics Report, University of Colorado, 1969 (unpublished).

[31]K. Maischberger, IEEE J. Quantum Electron. QE-7, 250 (1971).